

## Reparametrization of Karplus Equation Relating ${}^3J_{C-C-O-P}$ to Torsion Angle

Janez Plavec and Jyoti Chattopadhyaya\*

Department of Bioorganic Chemistry, Box 581, Biomedical Centre, Uppsala University, S-751 23 Uppsala, Sweden.

**Abstract.** A new three-parameter Karplus equation  ${}^3J_{C-C-O-P} = 9.1 \cos^2\Phi - 1.9 \cos\Phi + 0.8$  is based on the 17  ${}^3J_{CP}$  coupling constants and the corresponding X-ray derived torsion angles giving an r.m.s. of 0.3 Hz and  $\Delta J < 0.5$  Hz between  $J_{exp}$  and  $J_{calc}$ . An attempt is also made to relate  ${}^3J_{CP}$  to torsion angle and  $\alpha$ -carbon substituent electronegativity.

Conformational studies of nucleic acids using NMR methods consist of measurement of NOEs and coupling constants.<sup>1</sup> Proton-proton coupling constants are used to define sugar ring conformation, whereas several heteronuclear coupling constants reflect the phosphate backbone conformation. The determination of the torsion angle  $\epsilon[C4'-C3'-O3'-P3']$  requires the knowledge of three coupling constants  ${}^3J_{C4P3}$ ,  ${}^3J_{C2P3}$  and  ${}^3J_{H3P3}$ , whereas  $\beta[P5'-O5'-C5'-C4']$  is defined by  ${}^3J_{C4P5}$ ,  ${}^3J_{H5P5}$  and  ${}^3J_{H5''P5}$ . The prerequisite for the interpretation of vicinal carbon-phosphorous coupling constants ( ${}^3J_{CP}$ ) in terms of precise values of  $\epsilon^t$ ,  $\epsilon^-$  and  $\epsilon^+$  together with the respective molar ratio of rotamer distribution is the availability of high quality Karplus-type equation for C-C-O-P molecular fragments. Several parametrizations<sup>2-5</sup> of the eqn. 1 have led to different sets of (A,B,C) parameters:

$${}^3J_{CP} = A \cos^2\Phi + B \cos\Phi + C \quad \dots\dots (1)$$

The most recent reparametrization of eqn. 1 has been performed by Hilbers *et al.* [Fig. 1a, dotted (....) line].<sup>5</sup> These authors have observed  ${}^3J_{CP}$  of 11.1 Hz which could not be accounted for by the older (A,B,C) parameters in eqn. 1 developed by Altona *et al.* [Fig. 1a, dashed (----) line].<sup>4</sup> In both of these approaches<sup>4,5</sup> individual Karplus (A,B,C) parameters for  ${}^3J_{HP}$  and  ${}^3J_{CP}$  couplings together with the  $\Phi[C-C-O-P]$  torsion are iterated by least square fitting to obtain the best fit to experimental couplings. The use of only  ${}^3J_{CP}$  from fully stacked oligonucleotides in Altona and coworkers formulation<sup>4</sup> with  $\epsilon^t$  rotamers narrows the region of torsion angles to values  $\approx 220^\circ$  for  ${}^3J_{C4P3}$  and  $\approx 100^\circ$  for  ${}^3J_{C2P3}$ , which has been enlarged in the *trans* region with the introduction of  ${}^3J_{CP}$  characteristic for  $\beta^t$  rotamers.<sup>4</sup> Additionally, both of the above parametrizations of eqn. 1<sup>4,5</sup> have made use of one indirectly estimated calibration point at  $60^\circ$  (0.7 Hz). It is known<sup>4,5</sup> that the reliability and accuracy of Karplus curves is not fully straightforward when applied to the analysis of torsion angles below  $90^\circ$ . We have therefore deemed it essential to introduce as many experimental (combination of X-ray determined torsion and NMR determined  ${}^3J_{CP}$ ) calibration points as possible in the *gauche* region to improve the precision of parameters in Karplus eqn. 1. In this aspect we have here introduced the combination of NMR and X-ray data on 3',5'-cyclic nucleotides for which the vicinal  ${}^3J_{CP}$  coupling constants can be related to  $\Phi[C-C-O-P]$  torsions of  $\approx 60^\circ$  and  $\approx 300^\circ$ . <sup>1</sup>H NMR data has shown that cyclic phosphate ring in 3',5'-cyclic nucleotides which is *trans*-fused to the ribose moiety is locked into the chair conformation, and adopts similar conformation in solution and solid state,<sup>6,7</sup> which is not found to be the case for 2',3'-cyclic nucleotides.<sup>16</sup> The  ${}^3J_{C2P}$  of 3',5'-cyclic nucleotides were found in the range 7.8-8.3 Hz,<sup>8</sup> with  $[C2'-C3'-O3'-P3']$  torsion angles determined by X-ray crystallography around  $180^\circ$ .<sup>9</sup> These  ${}^3J_{C2P}$  are smaller by  $\approx 2-3$  Hz than the usual *trans* coupling constants observed in 3' $\rightarrow$ 5', 2' $\rightarrow$ 5' and other branched and lariat oligonucleotides<sup>17</sup> as a result of different bond distances and angles as well as electronegativities of the vicinal substituents along the coupling pathway, and they have therefore not been used in our parametrization of three-parameter Karplus eqn. 1.

**Table 1.** Experimental  $^3J_{CP}$  and the corresponding torsion angles in comparison with the calculated  $^3J_{CP}$  using modified Karplus eqns. 2 and 3.

No.	$J_{CP}$	Input experimental data				Results from modified Karplus eqns.			
		$J_{exp}^a$	$\Phi^a$	$\Delta\chi_1$	$\Delta\chi_2$	Eqn. 2 <sup>b</sup>	Eqn. 3 <sup>b</sup>	$J_{calc}$	$J_{calc} - J_{exp}$
1	J(C4'-P3')	7.8 (4)	219.5 (4)	0.4	0.0	7.7	-0.1	7.5	-0.3
2	J(C2'-P3')	1.8 (4)	99.5 (4)	0.0	0.4	1.4	-0.4	1.4	-0.4
3	J(C4'-P3')	7.9 (4)	217.0 (4)	0.4	0.0	8.1	0.2	8.0	0.1
4	J(C2'-P3')	1.3 (4)	97.0 (4)	0.0	0.4	1.2	-0.1	1.2	-0.1
5	J(C4'-P3')	8.1 (4)	214.5 (4)	0.4	0.0	8.5	0.4	8.5	0.4
6	J(C2'-P3')	0.7 (4)	94.5 (4)	0.0	0.4	1.0	0.3	1.1	0.4
7	J(C4'-P3')	6.0 (4)	226.5 (4)	0.4	0.0	6.4	0.4	6.2	0.2
8	J(C2'-P3')	2.1 (4)	106.5 (4)	0.0	0.4	2.1	0.0	2.0	-0.1
9	J(C4'-P5')	11.1 (5)	196.0 (5)	0.0	0.0	11.0	-0.1	11.1	0.0
10	J(C4'-P5')	11.1 (5)	164.0 (5)	0.0	0.0	11.0	-0.1	11.1	0.0
11	J(C4'-P3')	10.9 (10)	202.1 (11)	0.4	0.0	10.4	-0.5	10.5	-0.4
12	J(C4'-P5')	10.9 (10)	197.0 (11)	0.0	0.0	10.9	0.0	11.0	0.1
13	J(C4'-P3')	2.2 (8)	300.0 (9a)	0.4	0.0	2.1	-0.1	2.3	0.1
14	J(C4'-P3')	2.2 (8)	56.9 (9a)	0.0	0.0	2.5	0.3	2.2	0.0
15	J(C4'-P3')	2.3 (8)	299.0 (9b,c)	0.4	0.0	2.0	-0.3	2.2	-0.1
16	J(C4'-P3')	2.3 (8)	57.9 (9b,c)	0.0	0.0	2.4	0.1	2.2	-0.1
17	J(C2'-P3')	0.8 (10)	82.1 (11)	0.0	0.4	0.7	-0.1	0.9	0.1

<sup>a</sup>  $^3J_{CP}$  coupling constants are in Hz, torsion angles are in degrees and the original reference to the literature is given in parentheses.  $\Delta\chi_1$  and  $\Delta\chi_2$  are differences in the Huggins electronegativities<sup>15</sup> between the  $\alpha$ -substituents on positions 1 and 2,<sup>12,14</sup> respectively on the 'middle' carbon and hydrogen ( $\Delta\chi_i = \chi_i - 2.2$ ). <sup>b</sup> R.m.s. deviations between input and back-calculated  $^3J_{CP}$  values using eqns. 2 and 3 are 0.3 and 0.2 Hz, respectively.

We have utilized 8 calibration points used by Altona *et al.*<sup>4</sup> which were obtained by extrapolation of experimental  $^3J_{CP}$  to pure stacked conformational states (Entries 1-8 in Table 1). Four *trans*  $^3J_{CP}$ <sup>5,10</sup> and corresponding torsion angles are from high resolution molecular structure found by single crystal X-ray diffraction analysis<sup>11</sup> (Entries 9-12 in Table 1). Four *gauche*  $^3J_{CP}$  and torsion angles originate from NMR study<sup>8</sup> and X-ray structures of 3',5'-cAMP<sup>9a</sup> and 3',5'-cUMP<sup>9b,c</sup> (Entries 13-16 in Table 1). The experimental  $^3J_{CP}$  values<sup>8</sup> were divided by two due to two competing coupling pathways.<sup>3</sup> We believe that the error that such a simplified correction would introduce in our input data set is below the error of determination<sup>8</sup> of  $^3J_{CP}$  ( $\pm 0.25$  Hz). We have also included in our data set  $^3J_{CP}$  of 0.8 Hz (Entry 17 in Table 1) which is in the range where Karplus curve has a minimum. In original paper<sup>10</sup> this coupling constant was determined as  $<1.0$  Hz. In our least-square analyses the change of this  $^3J_{CP}$  to 0.3 or 0.5 Hz has made negligible change in (A,B,C) parameters of eqn. 1. A least square optimization using 17  $^3J_{CP}$  values and the corresponding torsion angles (Table 1) resulted in the following three-parameter Karplus equation:

$$^3J_{CP} = 9.1 \cos^2\Phi - 1.9 \cos\Phi + 0.8 \quad \dots\dots (2)$$

Plot of eqn. 2 as a function of  $\Phi$ [C-C-O-P] together with all 17 calibration points is shown in Fig. 1a [thick (—) line]. It is clear from both Fig. 1a and Table 1 that the resulting fit from the least squares optimization in eqn. 2 is very satisfactory: all input  $^3J_{CP}$  are reproduced within 0.5 Hz ( $\Delta J = J_{calc} - J_{exp}$ ) and r.m.s. deviation between input and back-calculated  $^3J_{CP}$  values is 0.3 Hz. Note that there is the large discrepancy between our eqn. 2 and the curves derived by Altona<sup>4</sup> and Hilbers<sup>5</sup> below  $90^\circ$  (compare the dotted- and dashed-line curves with our solid line in Fig. 1a). Notable is also the difference of  $\approx 3$ -4 Hz in the *cis* couplings ( $\Phi \approx 0^\circ$ ) amongst the three curves in Fig. 1a.

A three-parameter Karplus equation (eqns. 1 or 2) is applicable to limited class of compounds because factors such as bond distance, bond angle, substituents and orientation of neighbouring groups are implicitly

included in (A,B,C) parameter set. Hence, we have explored the further potential of eqn. 2 by examining the influence of electronegativity of  $\alpha$ -C and  $\alpha$ -H attached to the 'middle' carbon of C-C-O-P fragment on  ${}^3J_{CP}$  in eqn. 3.<sup>12</sup> The considerations described in note 12 have led us to set up five-parameter Karplus equation (eqn. 3),<sup>18</sup> which includes terms similar to generalized Haasnoot-Altona equation<sup>13</sup> (with parameters  $P_1 - P_6$ ) used in the analysis of  ${}^3J_{H-C-C-H}$ . The optimum values of five parameters in eqn. 3 were determined by the least-square conjugate gradient minimization using 17  ${}^3J_{CP}$  values, torsion angles and corresponding electronegativities of  $\alpha$ -substituents on 'middle' carbon (Table 1).

$${}^3J_{CP} = 6.9 \cos^2\Phi - 3.0 \cos\Phi + 1.8 + \sum_{i=1,2} \Delta\chi_i [-3.2 + 6.2 \cos^2(\zeta_i\Phi + |\Delta\chi_i|)] \quad \dots\dots (3)$$

The first three terms describe the torsion angle dependence of  ${}^3J_{CP}$ , while the last two parameters describe its dependence on the electronegativity of substituents.  $\Delta\chi_i$  is the difference in the electronegativity between  $\alpha$ -substituent and hydrogen in the Huggins scale.<sup>14</sup>  $\zeta_i$  is a parameter which denotes substituent's orientation ( $\zeta_1 = 1$ ,  $\zeta_2 = -1$ , see Newman projection in note 12).<sup>13</sup> Fig. 1b shows that the fit from the least square fit is indeed satisfactory which is evident from the fact that all input  ${}^3J_{CP}$  are reproduced within  $\Delta J \leq 0.4$  Hz with r.m.s. deviation of 0.2 Hz between input and back-calculated  ${}^3J_{CP}$  values (Table 1).

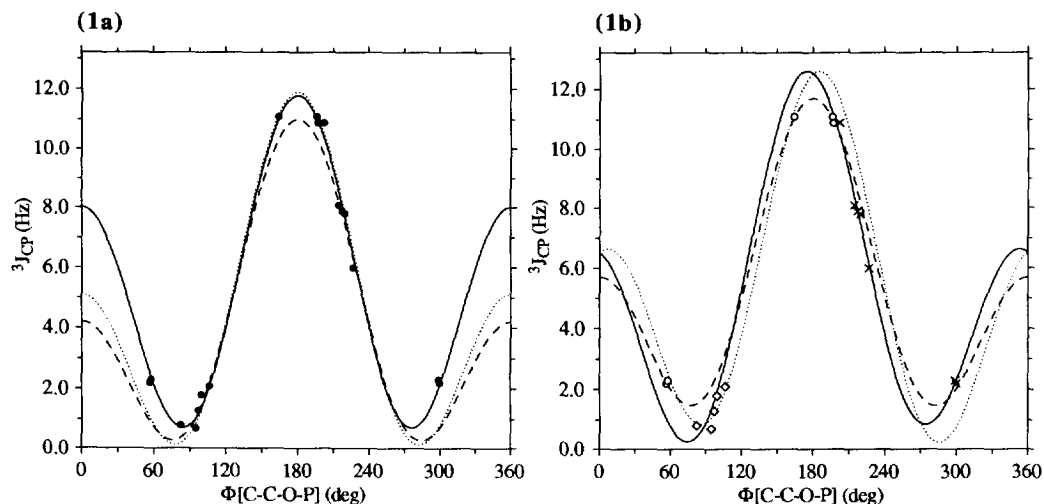


**Figure 1.** (1a). The plot of eqn. 2 (—) in comparison with the three-parameter Karplus equations derived by Altona *et al.*<sup>4</sup> (- - -, eqn. 1 with A=6.9, B=-3.4, C=0.7) and Hilbers *et al.*<sup>5</sup> (····, eqn. 1 with A=8.0, B=-3.4, C=0.5). The  ${}^3J_{CP}$ -torsion angle data points which were used in our parametrization are indicated by filled circles. (1b). The plot of eqn. 3 with different  $\Delta\chi_i$  values for  ${}^3J_{C_4P_3}$  (—,  $\Delta\chi_1 = 0.4$ ,  $\Delta\chi_2 = 0.0$ ),  ${}^3J_{C_2P_3}$  (····,  $\Delta\chi_1 = 0.0$ ,  $\Delta\chi_2 = 0.4$ ) and  ${}^3J_{C_4P_5}$  (- - -,  $\Delta\chi_1 = \Delta\chi_2 = 0.0$ ). The input calibration points used to obtain the best fit values of five parameters in eqn. 3 consist of three distinct sets (Table 1): (1) seven points with  $\alpha$ -C on position 1 ( $\Delta\chi_1 = 0.4$ ) and H on position 2 ( $\Delta\chi_2 = 0$ ) are shown by 'x', (2) five points with H on position 1 ( $\Delta\chi_1 = 0$ ) and  $\alpha$ -C on position 2 ( $\Delta\chi_2 = 0.4$ ) are shown by 'o' and (3) five points with two H on positions 1 and 2 ( $\Delta\chi_1 = \Delta\chi_2 = 0$ ) are shown by '•'.

Although a comparative evaluation of eqns. 3 and 2 showed the slight decrease in the deviation between experimental and calculated  ${}^3J_{CP}$  in the former (Table 1), we however issue clear warning against the uncritical use<sup>15</sup> of eqn. 3: (a) Input calibration points cover only small regions of torsion angle space especially as their torsions are further scattered according to their respective substituent electronegativities on the 'middle' carbon (see Fig. 1b for the three sets of input calibration points). (b) In our data set  $\alpha$ -substituents on the 'middle' carbon are C and H, which differ by only 0.4 units in Huggins electronegativity scale.<sup>14</sup> Clearly, to increase the

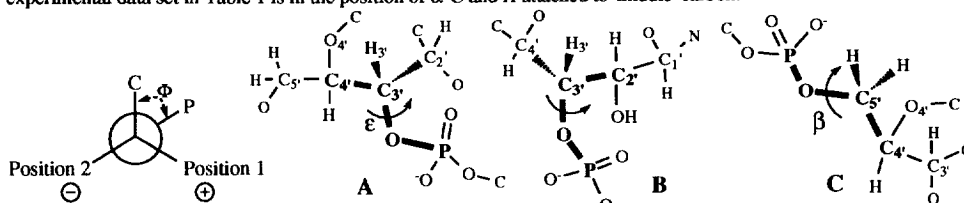
confidence and applicability of eqn. 3 a larger set of compounds with distinctly different substituents (like O and F) would be needed. (c) The signs of  $P_4$  and  $P_5$  (following the Haasnoot-Altona's notation) in eqn. 3 are reversed<sup>13</sup> in comparison with the respective parameters for  $^3J_{HH}$ , which means that more data points are needed to prove that the asymmetry of  $^3J_{CP}$  curve is indeed inverted relative to  $^3J_{HH}$ . Further work is in progress to unequivocally prove the influence of the electronegativity<sup>15</sup> on the relationship between  $^3J_{CP}$  and C-C-O-P torsion angles.

#### ACKNOWLEDGMENT

We thank Swedish Board for Technical Development (NUTEK) and Swedish Natural Science Research Council (NFR) for generous financial supports. We also thank the anonymous referee for pointing out some of the shortcomings of eqn. 3.

#### REFERENCES AND NOTES

1. Van de Ven, F.J.M.; Hilbers, C.W. *Eur. J. Biochem.* **1988**, *178*, 1.
2. Lapper, R.D.; Smith, I.C.P. *J. Am. Chem. Soc.* **1973**, *95*, 2880.
3. Davies, D.B.; Sadikot, H. *Org. Magn. Reson.* **1982**, *20*, 180.
4. Lankhorst, P.P.; Haasnoot, C.A.G.; Erkelens, C.; Altona, C. *J. Biomol. Struct. Dyn.* **1984**, *1*, 1387.
5. Mooren, M.M.W.; Wijmenga, S.S.; van der Marel, G.A.; van Boom, J.H.; Hilbers, C.W. *Nucl. Acids Res.* **1994**, *22*, 2658.
6. Blackburn, B.J.; Lapper, R.D.; Mantsch, H.H.; Smith, I.C.P. *J. Am. Chem. Soc.* **1973**, *95*, 2873.
7. Haasnoot, C.A.G.; de Leeuw, F.A.A.M.; de Leeuw, H.P.M.; Altona, C. *Org. Magn. Reson.* **1981**, *15*, 43.
8. Lapper, R.D.; Mantsch, H.H.; Smith, I.C.P. *J. Am. Chem. Soc.* **1973**, *95*, 2878. With reversed assignment of C3' and C4'.<sup>3</sup>
9. Torsion angles were extracted from the positional coordinates available in the Cambridge structural data base and their average is given in Table 1 for: (a) 3',5'-cAMP Na<sup>+</sup> (refcode 'NAAMPH10') Varughese, K.I.; Lu, C.T.; Kartha, G. *J. Am. Chem. Soc.* **1982**, *104*, 3398. (b) 3',5'-cUMP (refcode 'BEBVEJ' with all coordinates negated) Qitai, Z.; Shiqi, D.; Yuanxin, G. *Acta Phys. Sin.* **1981**, *30*, 1369. (c) 3',5'-cUMP Et<sub>3</sub>N<sup>+</sup> (refcode 'TEAURP10') Coulter, C.L. *Acta Crystallogr., Sect. B.* **1969**, *25*, 2055.
10. Blommers, M.J.J.; Haasnoot, C.A.G.; Walters, J.A.L.I.; van der Marel, G.A.; van Boom, J.H.; Hilbers, C.W. *Biochemistry* **1988**, *27*, 8361.
11. Frederick, C.A.; Coll, M.; van der Marel, G.A.; van Boom, J.H.; Wang, A.H.-J. *Biochemistry* **1988**, *27*, 8350.
12. Analysis of the coupling pathways of 17  $^3J_{CP}$ -torsion angle data points given in Table 1 shows that: (1)  $^3J_{C4P3}$  pathway has  $\alpha$ -C attached to 'middle' carbon on position 1 (see Newman projection below) which is likely to be influenced by  $\beta$ -substituents which are O, C and H in six cases (see the drawing A) and C and two H atoms in one case, (2)  $^3J_{C2P3}$  pathway has  $\alpha$ -C attached to the 'middle' carbon on position 2 with O, C and H as  $\beta$ -substituents in all five cases (see the drawing B), (3)  $^3J_{C4P5}$  pathway has two protons on the 'middle' carbon (see the drawing C), (4) the variation of the substituents on 'initial' carbon (see the drawings A-C) in our 17 point data set is negligible with  $\alpha$ -substituents being O, C and H in all but entry 17, (5)  $\beta$ -heteroatom substituents on 'initial' carbon of  $^3J_{C4P3}$  and  $^3J_{C2P3}$  pathways are O, C in the former and O,N in the later which is a small difference in terms of  $\Delta\chi_i$  (1.7 versus 2.15) that is not expected to considerably alter the electronegativity of  $\alpha$ -substituents. In conclusion, the main difference between coupling pathways contributing to  $^3J_{C4P3}$  and  $^3J_{C2P3}$  in our 17 point experimental data set in Table 1 is in the position of  $\alpha$ -C and H attached to 'middle' carbon.



13. Haasnoot, C.A.G.; de Leeuw, F.A.A.M.; Altona, C. *Tetrahedron* **1980**, *36*, 2783.
14. Huggins, M.L. *J. Am. Chem. Soc.* **1953**, *75*, 4123.
15. The plots of  $^3J_{C4P3}$ ,  $^3J_{C2P3}$  and  $^3J_{C4P5}$  using eqn. 3 as a function of systematic variation of the torsion angle in Fig. 1b show how  $^3J_{CP}$  changes as the  $\alpha$ -substituent electronegativity and its orientation change. In the *trans* region ( $\Phi \approx 180^\circ$ ) both  $^3J_{C4P3}$  and  $^3J_{C2P3}$  with  $\alpha$ -C substituent at 'middle' carbon in C-C-O-P molecular fragment are increased in comparison to  $^3J_{C4P5}$  with two protons. Similar effect was discussed by Davies<sup>3</sup> who has introduced electronegativity correction of  $^3J_{C1P}$  coupling by 1.1 Hz due to N substituent at the 'initial' carbon. In the *gauche* region ( $\Phi \approx 60^\circ$  and  $\approx 300^\circ$ ) in Fig. 1b,  $^3J_{C4P5}$  is larger than  $^3J_{C4P3}$  and  $^3J_{C2P3}$ , suggesting that  $^3J_{CP}$  is considerably reduced due to the incorporation of electronegativity of  $\alpha$ -substituents on the 'middle' carbon of the coupling pathway of C-C-O-P fragment.
16. Lapper, R.D.; Smith, I.C.P. *J. Am. Chem. Soc.* **1973**, *95*, 2880.
17. Sund, C.; Agback, P.; Koole, L.H.; Sandström, A.; Chattopadhyaya, J. *Tetrahedron* **1992**, *48*, 695.
18. The parameter  $P_6$  (according to the Haasnoot-Altona's notation<sup>13</sup>) has been kept frozen because only is such a way a unique set of five-parameters given in eqn. 3 could be obtained.